DETACHED DIVERTOR PLASMAS IN ALCATOR C-MOD: A STUDY OF THE ROLE OF ATOMIC PHYSICS

LIPSCHULTZ, B.*, BOSWELL, C.*, GOETZ, J.A.*, PITCHER, C.S.*, TERRY, J.L.*, WEAVER, J.L.**, WELCH, B.L.**†, HUBBARD, A.*, KRASHENINNIKOV, S.I.*, LABOMBARD, B. L.*, PAPPAS, D.A.*
*M.I.T. Plasma Science and Fusion Center, Cambridge, Ma., 02139, USA
**Institute for Plasma Research, U. Maryland, Maryland 20742, USA

Abstract

Detailed profiles of the volumetric recombination occurring in Alcator C-Mod plasmas are presented. During detachment the recombination sink is compared to the divertor plate sink as well as the divertor ion source. Depending on plasma conditions, volume recombination removes between 10 and 75% of the ions before they reach the plates. A second, equally important process that leads to a drop in plate ion current is inferred to be a reduction in divertor ion source, which is correlated with a drop in power flowing into the ionization region and the pressure loss of detachment. For high $\bar{n}_e$ the divertor recombination can cross the separatrix near the x-point, cool the core and lead to a disruption. Experimental measurements show a difference in ion and neutral velocities for H-mode detached plasmas. The resulting ion-neutral collisions are found to be more efficacious than recombination in removing momentum from the ions. The neutral component of volumetric power emission from the divertor has been measured by means of a novel filtering technique to be substantial (~ 20% of the total divertor volumetric emission).

1. INTRODUCTION

Finding ways of dissipating the SOL heat flux is a major thrust of magnetic fusion research. Dissipative divertor scenarios, such as the radiative and detached divertor (see for example [1,2] and references therein), are successful in lowering the temperatures at the divertor plates to ~ 1 - 5 eV [3,4]. At such low T_e's ion-neutral collisions and volume recombination become important in comparison to ionization [5-7]. This paper reports results of a study in which the roles of these processes as sinks for power, momentum, and ion flow to the divertor plates were investigated.

These measurements were made on the Alcator C-Mod tokamak. A general description of the diagnostics and characteristics of the device are contained elsewhere [8]. All data included in this paper were obtained with 5.3 T toroidal magnetic field and a lower x-point. Data are reported for discharges ranging from ohmic to ICRF-heated plasmas (both L- and H-mode confinement).

2. ION FLOW TO THE PLATES

Volume recombination has been shown to exist in divertor plasmas [9-18] but its contribution as a sink for ions, as evidenced by the reduction in ion flow to the divertor plates, is more difficult to quantify [9,11,13,15,16,18]. We examine here the magnitude and time-dependence relative to the rate of ions reaching the divertor plates and of the ion source during divertor detachment.

The Balmer and Lyman series spectra and nearby continuum emitted from recombining plasma regions are utilized to derive the local n_e, T_e, and volume recombination rate. These spectra are measured with visible [16,19] and VUV spectrometers [13,19]. The visible spectrometer can simultaneously monitor up to 16 inputs, corresponding to different chords within the views 'O' and 'T' of the plasma, Fig. 1. The VUV spectrometer has a single, nearly horizontal viewing chord, that can be scanned to look through the x-point and above. The primary characteristic of both Balmer and Lyman spectra is that the line intensities $I_{p \rightarrow q}$ are recombination-dominated, as evidenced by the fact that they decrease much more slowly for increasing p than in the case where the emission is produced by excitation from the ground state [13,19].

---

† present address Applied Research Center, 12050 Jeffereson Ave., Newport News, Va. 23606.

To determine the recombination rate we need first to identify the basic characteristics of the recombining region. The techniques used are described elsewhere [13,15,16,19]. Typical visible and VUV recombining spectra are shown in Fig. 2. The widths of the Stark-broadened Balmer lines are a measure of n_e. A fit of a Saha-Boltzmann distribution to the p=5-8 Balmer lines gives T_e. Both n_e and T_e can also be derived from the VUV continuum at $\lambda \leq 91$ nm, Fig. 2(b). The opacity of the plasma to the Lyman series emission is estimated by the measurement of D_α/Ly_β and a radiative transfer model. The modeling also shows that in these plasmas, trapping reduces the recombination rate by a factor ~5 relative to the optically-thin case.

The primary method of estimating the volume recombination rate is based on a formalism described in a previous work [13,15] that allows one to determine the recombination rate, given knowledge of the emitting region n_e, T_e, any D^0 line brightness, and opacity to the Lyman series. Due to lack of D_α/Ly_β measurements for all discharges and locations, we have conservatively assumed in this analysis that the highest measured levels of opacity exist everywhere in the divertor. This potentially leads to a significant underestimate (~ factor of 2) of the volume recombination rate.

Results of the above analyses for a typical discharge, utilizing the Dγ line brightness, are given in Fig. 3. These data are from view 'O' of Fig. 1 where the viewing chords are almost perpendicular to the outer divertor plate surface. Each chord provides information about the plasma characteristics from the dominant emission region along the viewing chord located at a particular height z above the strike point (z=0). For reference, the outer divertor 'nose' (see Fig. 1) is at z ~ 5 cm. Divertor detachment, identified as a localized pressure loss at the plate compared to upstream, starts at ~ 0.6 seconds and spreads across the viewing region until ~ 0.8 seconds, when the entire region is detached. The core density is increasing up until 1.0 seconds. Even in the initial time frame shown, before pressure loss is observed, there is a high n_e (3a), low T_e, (3b), recombining region (3c) in the field of view. The probe measurements at the plate surface show T_e there to be higher (4-10 eV) and a range in n_e ($0.2\text{-}1.x10^{21} m^{-3}$) implying that the plasma characteristics shown in the initial time are likely from the private flux region. As time increases, the peak n_e and recombination rate increase and the recombining region expands across the separatrix and up the plate. At 1.1 seconds a significant amount of recombination is occurring in regions above the field of view 'O' and is then monitored by the second view 'T'.

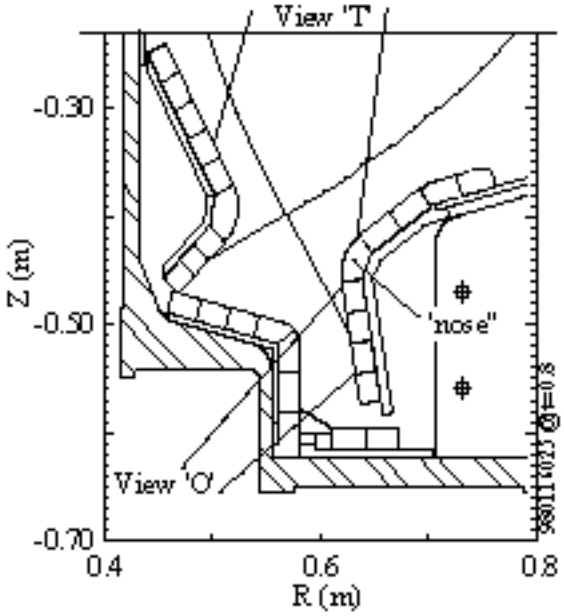

Figure 1: The Alcator C-Mod divertor region. View 'O' includes 7 chordal views of the outer divertor. View 'T' includes 8 chordal views. Viewing chords have < 1 cm spatial resolution.

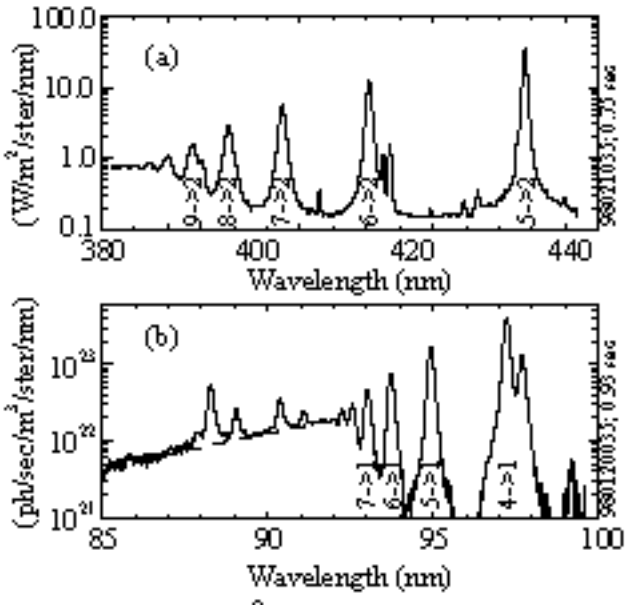

Figure 2: Typical D^0 recombining spectra in the visible (a) and VUV (b). Dashed line represents a radiative recombination model w/emission region length ~ 1.5 cm, n_e~$1.8x10^{21}$ m^{-3}, T_e=0.7 eV.

The profiles of recombination obtained from views 'O' and 'T' can be spatially integrated to obtain the volume recombination sink (I_R) in the region of the inner or outer divertor (or total). We have made assumptions of toroidal symmetry and selected a poloidal plane of integration; the divertor surface for view 'O' and a horizontal plane through the x-point for view 'T'. We also integrate the ion saturation current obtained from divertor probes across the divertor surface to obtain the plate ion sink (I_P). The total ion sink (also source) is then $I_S \equiv I_R + I_P$. These integrals over just the outer divertor are shown in Fig. 4a for the same ohmic discharge shown in Fig. 3. The outer divertor plate current, I_P, starts decreasing at ~0.73 seconds, ultimately dropping to ~25% of its peak level. The local drop in ion current can be larger (≥10) and is simultaneous with local drops in pressure starting at ~0.6 seconds. Recombination (I_R) increases before detachment **and** before any clear loss in I_P. The I_R increase during the discharge is not equal to the drop in I_P. Thus the total ion source, I_S, decreases during detachment. By the end of the shot most ions (~75%) created in the divertor recombine before reaching the divertor plate.

The drop in ion source is potentially very significant. Scalings based on a 'two-point' model (e.g. Ref. [20]) for **attached** plasmas would predict that the total ion source should scale as $n_e^2/P_{SOL}^{3/7}$ where n_e is the density upstream in the SOL and P_{SOL} the power flowing across the separatrix. If we assume that $n_e^2 \quad \bar{n}_e^2$, then there is a drop in ion source to ~ 50% of its predicted attached value. This further emphasizes that the drop in I_P is due **both** to a increase in I_R and a decrease in I_S. The magnitude and time behavior of I_P, I_R, and I_S are similar for the inner divertor.

The drop in ion source correlates with changes in power flowing into the ionization region as well as momentum loss from the plasma. To illustrate the former effect we show two other detached discharges, Fig. 4b-c. The discharge shown in Fig. 4b is similar to that shown in Fig. 3 and 4a until ICRF heating is added at 0.9 seconds. The divertor then reattaches over most of the plate and I_P increases above ohmic attached values (with constant $\bar{n}_e$). From comparison of multiple divertor views we find that the recombination region shrinks and moves back to the plate even as I_R decreases

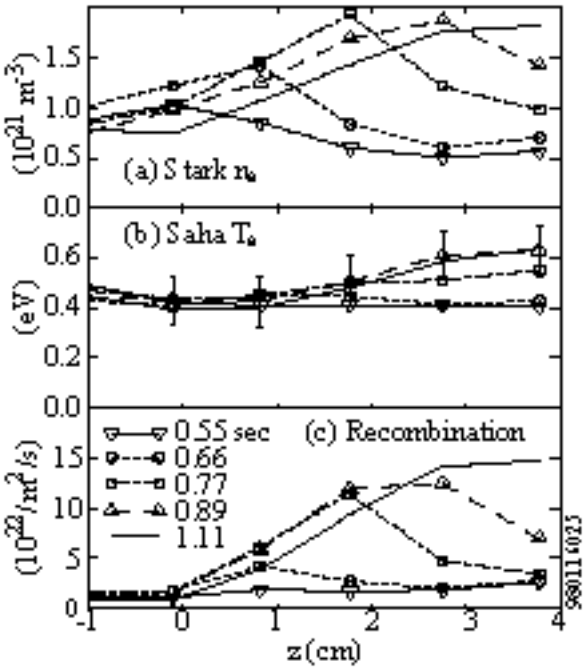

Figure 3: Evolution of the outer divertor characteristics. (a) n_e profiles derived from Stark broadening of Balmer 8→2 line; (b) T_e derived from fit of Saha distribution to Balmer population densities (5→8); (c) Local recombination rate based on n_e, T_e, D_γ intensity, assumptions of opacity, and recombinations/photon factor [13].

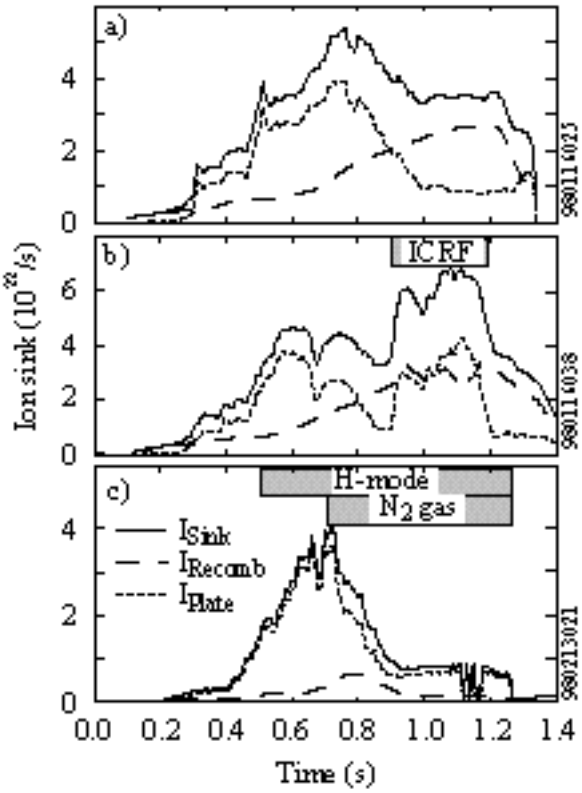

Figure 4: Outer divertor ion sinks for (a) Ohmic, (b) ICRF heating of detached plasma; and (c) detachment of an H-mode plasma with N_2 gas.

only slightly in magnitude! Close examination of the plasma characteristics indicates that the local volume recombination rate increases due to local increases in n_e. The primary effect of **adding** power to a detached discharge was to increase the ion source. In Fig. 4c we see the effect of **decreasing** the power flowing into the ionization region. N_2 gas is added at 0.7 seconds to an attached H-mode discharge. The ion current to the outer divertor plate and local plasma pressure both start decreasing shortly after the N_2 gas feed is initiated while $\bar{n}_e$ is held constant. However, there is little or no volume recombination (~10% of I_S). This emphasizes that a strong recombination sink is not necessary to reduce the ion current to the plates. Experimentally, decreasing the ion source is as effective as increasing volumetric recombination for decreasing the flow of ions to the divertor plates.

It is difficult to determine which regions of the divertor are affected by recombination from just the chordal integral data shown in Figures 3-4. We follow changes in the recombination region characteristics by imaging Dγ emission from the divertor with a CCD camera. Those Dγ images are then inverted by a singular value decomposition method [21,22], to provide local emissivities. Fig. 5 provides snapshots of the emission from a discharge where $\bar{n}_e$ increases until 1.0 second. In Fig. 5a detachment has just started and the recombination is concentrated near the plate ($\bar{n}_e=1.9\times10^{20}m^{-3}$). As the density is increased, the recombination region expands along flux surfaces away from the divertor plate towards the x-point and the midplane SOL, Fig. 5b ($\bar{n}_e=3.0\times10^{20}m^{-3}$). This expansion occurs both in the private and common flux regions and corresponds to flux surfaces that impact the outer divertor plate below the 'nose' (see Fig. 1) and are 'detached'. Finally, in Fig. 5c, the discharge has reached the highest core density, a value of $\bar{n}_e=3.3\times10^{20}m^{-3}$, almost twice the detachment threshold ($1.8\times10^{20}m^{-3}$) for this 800 kA ohmic discharge. There are two recombination regions, one in the divertor and a second INSIDE the separatrix, reaching 4 cm above the x-point. The corresponding midplane location for this region is 0.4 cm inside the separatrix. The recombination-dominated character of this 'x-point MARFE' is very similar to that recently identified for the MARFE at the inner midplane [19].

The existence of a second cold (< 1eV) and dense ($\sim1.5\times10^{20}m^{-3}$) recombining region inside the separatrix leads to effects on core radiation and the T_e profile. In Fig. 6(a) the time behavior of the principal VUV line intensities are shown for a chord passing through the upper edge of the x-point MARFE. The O^{5+} (145 eV ionization energy) line intensity peaks and decreases after 0.7 seconds. The sequential peaking and drop of successively lower-energy charge states of N and D imply that the local T_e is dropping precipitously from ~ 50-70 eV → ~5 eV. The plasma above the x-point becomes so cold that D line radiation is dominant. An ECE measurement of T_e 2 cm inside the separatrix at the midplane mirrors this cooling effect, Fig. 6(b). The discharge terminates when the x-point MARFE moves from the x-point to the inner wall and spreads poloidally. All of this occurs at a density corresponding to ~60% of the Greenwald limit [23].

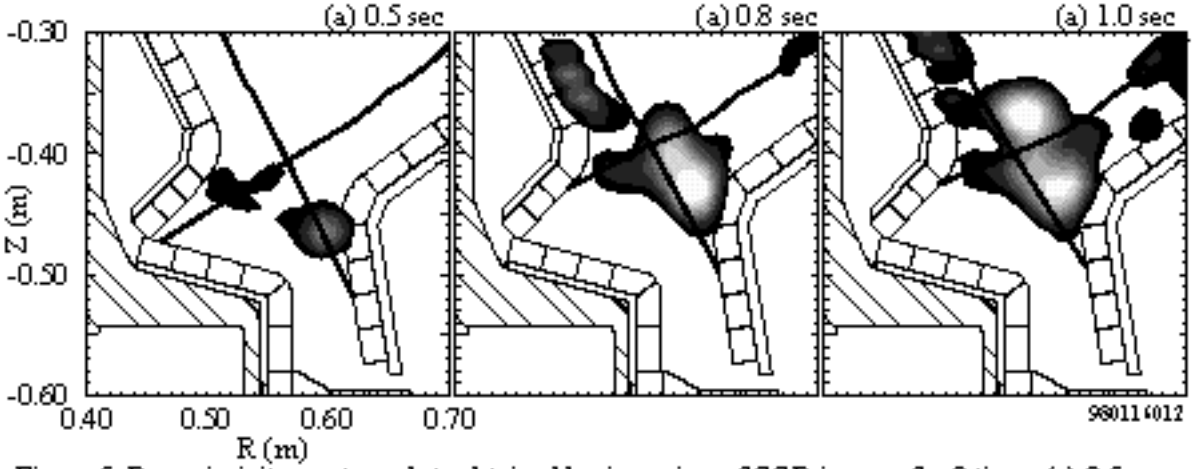

Figure 5: D_γ emissivity contour plots obtained by inversion of CCD images for 3 times (a) 0.5 sec., $\bar{n}_e=1.9\times10^{20}m^{-3}$ shortly after the start of detachment; (b) 0.8 sec., $\bar{n}_e=3.0\times10^{20}m^{-3}$; and (c) $\bar{n}_e=3.3\times10^{20}m^{-3}$. Maximum contour $5kW/m^2$. Each contour step $0.62\ kW/m^2$.

With the geometric information provided by the CCD images of Fig. 5 we can attempt to compare the relative magnitude of I_R (only the divertor recombination) and I_P over a number of discharges with varying $\bar{n}_e$, Fig. 7. As expected, the plate current peaks, and then falls as $\bar{n}_e$ is increased past the detachment threshold ($\bar{n}_e$=1.8x10^{20}m^{-3} for 0.8 MA, =2.2x10^{20}m^{-3} for 1 MA). The story is slightly more complicated for I_R. For both 0.8 and 1.0 MA discharges I_R increases linearly through the detachment threshold until I_P starts to asymptote to a minimum. The 0.8 MA discharges are then characterized by a saturation in the recombination level as the x-point MARFE begins forming ($\bar{n}_e$=2.5x10^{20}m^{-3}) and $\bar{n}_e$ is further increased. The x-point MARFE is just beginning to form in 1 MA discharges and the saturation in I_R is not clear in that case.

3. MOMENTUM LOSS

The loss in plasma pressure at the divertor plates is a primary characteristic of detachment. Both recombination and ion-neutral collisions (charge-exchange and elastic) transfer momentum from ions to neutrals. We can express these momentum losses as

$$d/dx[p_i + p_e + mnv^2] = -m(v-v_H)S_{i\text{-}n} \; -m(v)S_r \qquad (1)$$

x is along the magnetic field line, $p_{i,e}$ are the ion and electron static pressures ($T_i = T_e$ is assumed), m is the ion mass, n and v are the plasma density and velocity, and v_H is the neutral velocity. $S_{i\text{-}n} = nn_H\langle\sigma v\rangle_{i\text{-}n}$ and $S_r = n^2\langle\sigma v\rangle_r$ are the charge-exchange and recombination rates. The transfer of momentum to the walls is the same for either process; perpendicular transport of parallel momentum through i-n and n-n collisions (for the i-n mean free path smaller than the plasma fan width). In this section we try to estimate the role of i-n collisions as a sink for ion momentum in detached H-mode plasmas and compare it to that of recombination (based on section 2).

Ion-neutral collisions are only effective as a momentum sink if the relative velocity of the two species is non-negligible. We have addressed this question by comparing the Doppler shifts ofneutral atoms (D_α) and various ions (B-II, He-II), respectively, as measured with a high-resolution visible spectrometer [24]. Fig. 8a shows the loss in pressure at the plate relative to upstream for an H-mode plasma similar to that of Fig. 4c. H-mode starts at 0.52 seconds. N_2 gas is injected at 0.7 seconds followed shortly by detachment (loss in pressure). The corresponding ion and neutral velocities are

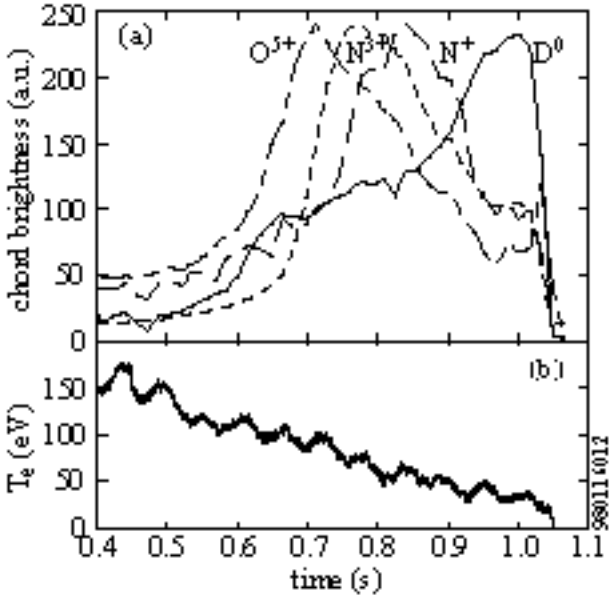

Figure 6: (a) VUV Brightness from a horizontal chord through the upper edge of the recombination region (Fig. 5c); all normalized to the same level. (b) T_e, 2 cm inside the separatrix, measured by ECE.

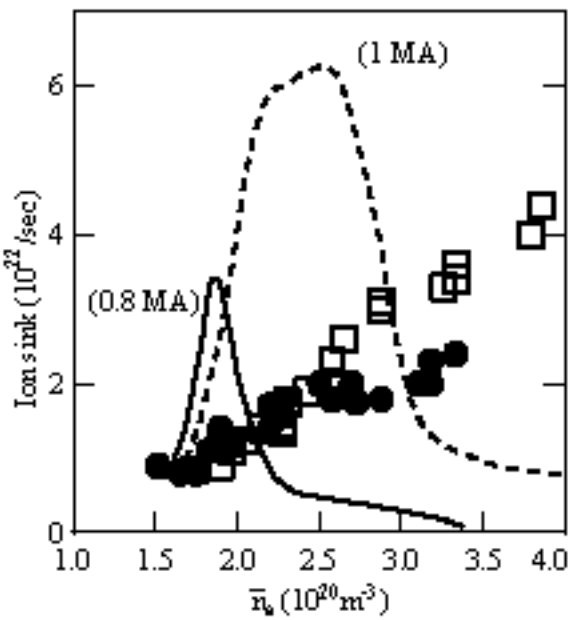

Figure 7: Recombination and plate ion sinks for two different plasma currents vs. $\bar{n}_e$. 0.8MA: Ip (——), I_R (●); 1MA Ip(– –), I_R (□).

shown in Fig. 8b with the ratio D_γ/D_α (photon rates) in Fig. 8c. The latter is provided asan indicator of the dominance of either excitation or recombination in determining the D_α brightness [10,14]. If excitation (recombination) dominates, then the D_α Doppler shift corresponds to the neutral (ion) velocity. For the ohmic detached C-Mod plasmas of Figures 3 and 4a, $D_\gamma/D_\alpha \geq 0.35$ corresponding to a low T_e (~0.5 eV) high n_e ($1x10^{21}m^{-3}$) recombining region and thus D_α is a measure of the ion velocity for those discharges. On the other hand, for the detached H-mode plasmas of Fig. 8, the opposite is true - D_γ/D_α is low and very little recombination is contributing to the D_α brightness (~ 10%). The resultant **neutral** velocities are measurably lower than the ion velocities (He-II). Such differences in velocities between neutrals and ions makes the momentum transfer very efficient in this region.

4. NEUTRAL POWER LOSS

Neutrals can potentially play an important role as an energy sink as well. We present here initial measurements of neutral power emission from the divertor region using a new filtering technique [26,27]. The detectors used are standard metal-film bolometers as developed for use on ASDEX [28]. They are sensitive to radiation (E < 5 keV) as well as neutrals that are absorbed in the foil. In order to 'filter' out the neutral component we inject neutral D_2 or He into the bolometer camera housing to raise the pressure there to ~ 200 mTorr. At such pressures the mfp for small-angle scattering (a few mm) is much shorter than the distance a neutral must travel through the high-pressure region to reach the bolometer foils and be absorbed (~4 cm). The presence of such high neutral densities in the bolometer camera leads to changes in the bolometer sensitivity (~15%) and cooling of the foils by heat conduction through the gas to the surrounding housing (~10% of a typical signal). These are both taken into account in this analysis.

This technique has been used to study a set of ICRF-heated detached L-mode discharges similar to that of Fig. 4b. Three such discharges are shown in Fig. 9; two with neutral filtering starting at ~0.5 seconds, one discharge without filtering (solid line). The ICRF heating period during which the divertor plasma reattaches over most of the plate, is labeled. The neutral component remains at a

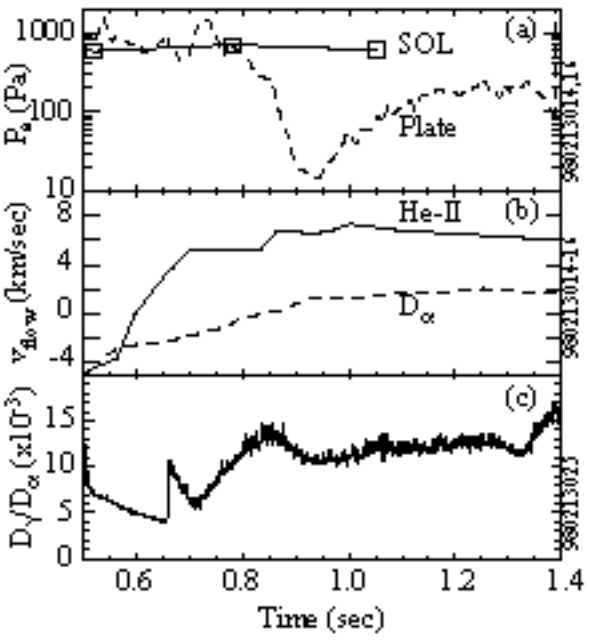

Figure 8. Detached H-mode characteristics: N_2 gas feed starts at 0.7 sec; detachment starts at ~0.8 sec.: a) Electron pressure in SOL (——) and at the plate (– –); (b) v_{flow} towards plate for He-II (——) and D_α (– –); c) D_γ/D_α ratio.

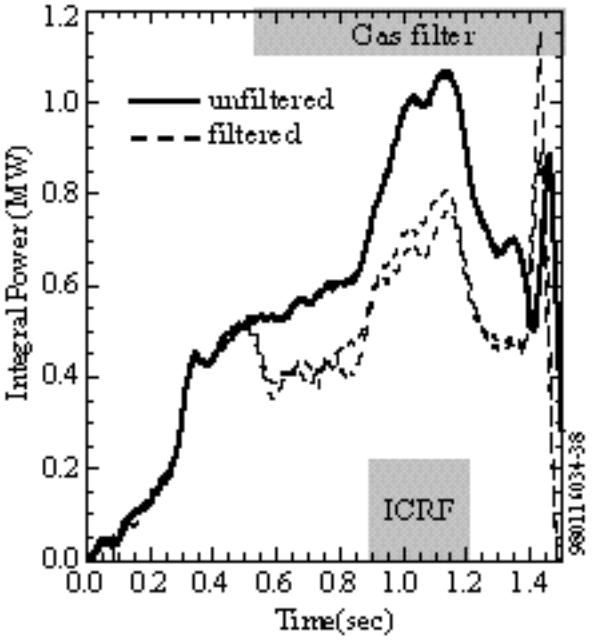

Figure 9. Integrated bolometer signal from the divertor with (– –) and without (——) neutral gas filtering. Detachment starts at 0.6 sec for this L-mode shot. The ICRF power causes reattachment over most of the divertor plate.

fairly constant fraction (~20%) of the total integrated emission through both ohmic detached, and partially reattached periods. The emission is peaked on bolometer chords aimed in the vicinity of the x-point or below. A simple model [29] of the neutral component of power and particle fluxes predicts that the neutral power flow should be 0.3-0.5x the D^0 radiated power. Based on the above measurements the impurities would then account for 0-40% of the divertor volumetric power losses. This appears low and at odds with previous measurements [1]. It is possible that some aspect of the model and/or analysis needs to be improved.

5. DISCUSSION

5.1 Loss of ion current

The large range in recombination levels of detached plasmas relative to the total ion sink (10-75%) is striking. This variation implies that the level of recombination is not a determining factor for detachment while at the same time it can still be a strong sink for ions. The existence of recombination before detachment points towards the possible existence of a dense cold detached region in the private flux zone prior to moving across the divertor leg to the plates.

The growth of the recombination region as the plasma density is increased past the detachment threshold can have important consequences for the core plasma. The x-point MARFE that forms at the highest densities cools the plasma just inside the separatrix and can lead to a disruption. This phenomenon may lead to further insight into density limits.

The results shown in this paper emphasize that we must pay attention to the ion source as well as sinks. We must explain - without the necessity of invoking a strong recombination sink - how the ion source and sink of particles (I_S) can decrease in detachment. To aid in this discussion we display two forms for the scaling of ion source:

$$eI_S x(20\ eV + \varepsilon + \gamma T_e) = P_{SOL} - P_{RAD,Z} + eI_R x \gamma T_e \qquad \textbf{(2)}$$

$$I_S \quad n_e^2 \bullet P_{SOL}^{-3/7} \bullet f_{mom}^2 \qquad \textbf{(3)}$$

Equation (2) is based just on energy considerations [16]. The basic 'two-point' model scaling mentioned earlier has been extended here [eq. (3)], by the f_{mom} term [$=(n_e T_e)_{DIV}/n_e T_e)_{SOL}$], for detached regimes [30]. ε is the ionization potential, P_{SOL} and $P_{RAD,Z}$ are the power flowing into the SOL and radiated by impurities respectively, and γ the sheath heat transmission coefficient. The I_R term in eq. (2) should be small compared to the terms on the LHS and so we can ignore it for this discussion. **Before** detachment (f_{mom}=1), Eq. 3 predicts that a decrease in P_{SOL} should **increase**, not decrease I_P, exactly the dependence we see in Fig. 3a. Equations (2) and (3) are consistent through the strong implicit dependence of T_e on n_e and P_{SOL} enforced by the condition of pressure constant on a flux surface.

After detachment, the terms in parentheses of eq. (2) are no longer dominated by γT_e and eq. (2) predicts a linear relation between eI_S and $P_{SOL} - P_{RAD,Z}$. The decrease in f_{mom} during detachment can lead to decreases in I_S.

Let us return to the discharges shown in Fig. 4a-c where we will be addressing the total effect on both divertors. In the first discharge [4(a)] the above equations would predict that as $\bar{n}_e$ is increased the ion source should also increase until detachment. Then, as $\bar{n}_e$ is increased still further (holding $P_{SOL} - P_{RAD,Z}$ ~ constant) eq. (2) would predict that the ion source should stay ~ constant. Again this seems consistent with Fig. 4a. The increase or decrease in ($P_{SOL} - P_{RAD,Z}$) [fig 4(b) and 4(c)] correspondingly increases or decreases I_S, again consistent with the above equations. A more quantitative analysis is presented elsewhere [16, 31].

5.2 Momentum loss

The ability to measure the neutral and ion velocities has given support to the importance of i-n collisions in removing momentum from the ion fluid. In addition, these measurements allow us to compare the relative efficacy of recombination and i-n neutral collisions in transferring momentum

to the neutral population. The ratio of recombination to i-n collision momentum transfer rates [25] is:

$$R \equiv [\langle\sigma v\rangle_r]/[\ (1-v_H/v)(n_H/n)\langle\sigma v\rangle_{i\text{-}n}] \qquad (4)$$

Using the measured velocities and recombination parameters that maximize $\langle\sigma v\rangle_r$ (opaque ohmic plasmas - Fig. 3a-b), R is close to 1 only for unrealistically low values of n_H/n ($\sim 5\times10^{-4}$) in the divertor. The above equation assumes that the regions over which recombination and i-n collisions remove momentum are identical. In reality, i-n collisions can act over significantly larger regions. The implication is that i-n collisions are likely to dominate the transfer of ion momentum to neutrals. The diffusion of momentum out of the plasma fan also carries energy as evidenced by the neutral power measured by the bolometers (section 4).

6. SUMMARY

The measurements presented here indicate that the loss of plate ion current during detachment is due to both an increase in recombination (ion sink) and a decrease in ion source/sink. The latter is consistent with decreases in energy available for ionization as well as increases in friction. During detachment, volume recombination can account for up to 75% of the total ion sink (source) in ohmic plasmas. Volume recombination increases as the detached region expands along and across flux surfaces and the ion current decreases. At the highest densities, in ohmic plasmas, we see that divertor detachment can lead to an x-point MARFE, core cooling and a plasma disruption. In H-mode plasmas where detachment is brought about by increasing radiative losses, the recombination ion sink is ≤ 10% of the ion source. High levels of recombination are thus not a necessary condition for detachment.

A significant difference in ion and neutral velocities, necessary for efficient removal of momentum, has been observed in some H-mode discharges. This gives further support to the basic models of momentum removal by ion-neutral collisions. An estimate of the relative role of recombination and i-n collisions in making the initial transfer of momentum from the ion fluid has been made. It appears that i-n collisions are more effective in momentum transfer for $v_H/v_{ion}<1$. In any case i-n collisions are responsible for transferring the momentum to the walls.

Based on a novel neutral filtering technique applied to bolometers we find that neutrals appear to also be an important vehicle for transfer of energy out the divertor plasma.

Acknowledgments

The authors wish to thank the entire Alcator group for assistance in acquiring this data. In particular we appreciate the calculations provided by S. Wukitch regarding RF power balance. We also thank Prof. P.C. Stangeby and Dr. G.M. McCracken for invaluable discussions. This work was supported by the U.S. D.oE. under contract #DE-AC02-78ET51013.

References

[1] GOETZ, J.A., KURZ, C., LABOMBARD, B., et al., Phys. Plasmas **3** (1996) 1908.
[2] PITCHER, C.S., STANGEBY, P.C., Plas. Phys. & Contr. Fus. **39** (1997) 779.
[3] LABOMBARD, B., GOETZ, J.A., KURZ, C., et al., Phys. Plasmas **2** (1995) 2242.
[4] ALLEN, S.A., HILL, D.N., CARLSTROM, T.N., et al., Plasma Phys. & Control. Fusion **37** (1995) A191.
[5] STANGEBY, P.C., Nucl. Fusion **33** (1993) 1695.
[6] KRASHENINNIKOV, S.I., et al., Phys. Plasmas **2** (1995) 2717.
[7] BORASS, K., COSTER, D., REITER, D., SCHNEIDER, R., J. Nucl. Mater. **241-243** (1997) 250.
[8] HUTCHINSON, I.H., BOIVIN, R., BOMBARDA, F., et al., Phys. Plasmas **1** (1994) 1511.
[9] LUMMA, D., TERRY, J.L., LIPSCHULTZ, B., Phys. Plasmas **4** (1997) 2555.
[10] ISLER, R., MCKEE, G.R., BROOKS, N.H., et al., Phys. Plasmas ibid., 2989.
[11] TERRY, J.L., LIPSCHULTZ, B., LABOMBARD, B., PAPPAS, D.A., Proc. of the 24th Euro. Conf. on Contr. Fus. and Plasma Phys., Berchtesgarden, Germany, June 1997, P2.022.

[12] NAPIONTEK, B., WENZEL, U., BEHRINGER, K., et al., ibid., Paper P4.008.
[13] TERRY, J.L., LIPSCHULTZ, B., PIGAROV, A. Yu. et al., Phys. Plasmas **5** (1998) 1759.
[14] MCCRACKEN, G.M., STAMP, M.F., MONK, R.D. et al., Nucl. Fusion **38** (1998) 619.
[15] TERRY, J.L., LIPSCHULTZ, B., et al., 13th Conf. on Plasma Surface Interactions in Controlled Fusion, 18-22 May, 1998, San Diego, Ca., paper I-1, accepted to J. Nucl. Mater.
[16] LIPSCHULTZ, B., TERRY, J.L., BOSWEL, C., et al., ibid., paper O-28, accepted to J. Nucl. Mater.
[17] MCCRACKEN, G.M., HORTON, L., LINGERTAT, J., et al., ibid., paper I-2, accepted to J. Nucl. Mater.
[18] WENZEL, U., BEHRINGER, K., CARLSON, A., et al., ibid. paper 3P-51, and Proc. of the 25th Euro. Conf. on Control. Fusion and Plasma Phys., Prague, Czech Republic, June 1998, Paper P2.010.
[19] LIPSCHULTZ, B., TERRY, J.L., BOSWELL, et al., Phys. Rev. Lett. **81** (1998) 1007.
[20] LOARTE, A., MONK, R.D., MARTIN-SOLIS, J.R., Nucl. Fusion **38** (1998) 331.
[21] FENSTERMACHER, M., ALLEN, S.L., BROOKS, N.H., et al., Phys. Plasmas **4** (1997) 1761.
[22] ALLEN, A., MIT Plasma Science & Fusion Center report PSFC/RR-97-1, Feb. 1997.
[23] GREENWALD, M., TERRY, J.L., WOLFE, S.M., et al., Nucl. Fusion **28** (1988) 2199.
[24] WELCH, B.L., WEAVER, J.L., GRIEM, H.R., et al., submitted to Phys. Plasmas.
[25] PITCHER, C.S., GOETZ, J.A., LABOMBARD, B., et al., 13th Conf. on Plasma Surface Interactions in Controlled Fusion, 18-22 May, 1998, San Diego, Ca., paper 2P-66, accepted to J. Nucl. Mater.
[26] GOETZ, J.A., et al., invited paper at 40th meeting of the Amer. Phys. Soc. Div. Plas. Phys. New Orleans, Nov. 1998, submitted to Phys. Plasmas.
[27] PITCHER, C.S., GOETZ, J.A., LIPSCHULTZ, B. et al., to be submitted to Rev. Sci. Instrum.
[28] ANDELFINGER, C., MAST, F., SCHRAMM, G., et al., in *Proceedings of the 15th Symposium on Fusion Technology*, Utrecht, The Netherlands, 19-23 September 1988 (Elsvier, Amsterdam, 1989), Vol. 1, p. 374.
[29] KRASENINNIKOV, S.I., accepted to Chec. J. of Plasma Physics.
[30] STANGEBY, P.C., 'The Plasma Boundary of Magnetic Confinement Devices', to be published by the Institute of Physics.
[31] LIPSCHULTZ, B., TERRY, J.L., et al., APS invited paper Nov. 98 New Orleans.